Vol. 12, No. 4, 2021
ISSN 2233-4203/ e-ISSN 2093-8950
ARTICLE www.msletters.org | Mass Spectrometry Letters

Li^+ and $Li^+I^-Li^+$ ions Solvated by 1,4-dioxane: An ion Mobility Spectrometry-Mass Spectrometry Study

Yunseop Choi, Inyong Ji, and Jongcheol Seo*

Department of Chemistry, Pohang University of Science and Technology (POSTECH), Pohang 37673, Korea

Received November 29, 2021; Revised December 13, 2021; Accepted December 13, 2021
First published on the web December 31, 2021; DOI: 10.5478/MSL.2021.12.4.152

Abstract : Electrospray ionization (ESI) and ion mobility spectrometry-mass spectrometry (IMS-MS) were employed to investigate the solvated structures of ionic species in the lithium iodide electrolyte solution in the gas phase. The $Li^+I^-Li^+$ triple ion and single standalone Li+ ions solvated by 1,4-dioxane were successfully generated and observed by ESI-MS under the influence of dioxane vapor at the inlet region. Under the present experimental condition, $(1,4\text{-dioxane})_m{\cdot}Li^+$ complex ions (m = 1, 2, and 3) and a $(1,4\text{-dioxane}){\cdot}Li^+I^-Li^+$ complex ion were observed, which were further examined by IMS to investigate their structures. The presence of multiple structural isomers was confirmed, which accounts for the endothermic conformational transition of 1,4-dioxane from a chair to a boat to achieve bidentate O-donor binding to Li^+ and $Li^+I^-Li^+$. Further structural details critical for the ion-solvent interactions were also examined and discussed with the help of density functional theory calculations.

Keywords : triple ion, ion solvation, lithium electrolyte, ion mobility spectrometry

Introduction

Electrolyte solutions contain large amounts of ionic and neutral molecules, in which neutral solvent molecules can dynamically solvate various ionic species. In the dilute solution, dissolved electrolytes may exist as solvated single cation or anion, but the ionic clusters with contact pairs of cations and anions can be generated and solvated under the increased electrolyte concentration.[1-3] Investigating the solvation energetics and structures of such ionic clusters are of fundamental importance because they considerably affect the ion transport properties (i.e., ion conductivity) in the electrolyte solution, which may be pivotal for their electrochemical applications as well as energy storage/ conversion systems.

Open Access
*Reprint requests to
https://orcid.org/0000-0001-5844-4585
E-mail: jongcheol.seo@postech.ac.kr.

This Article is dedicated to Professor Seung Koo Shin in commemorating his retirement and contribution to the Korean Society for Mass Spectrometry.

Among various ionic clusters, ionic clusters in lithium electrolytes and their solvation with O-donor solvents have been actively investigated due to their fundamental importance toward understanding ionic transport properties in the lithium-ion battery electrolyte.[4] Especially, many experimental and theoretical efforts have been made to understand solvation behaviors of lithium electrolyte ions and their triple ions ($Li^+X^-Li^+$ or $X^-Li^+X^-$),[5–13] since Torell and coworkers first claimed the formation of $Li^+CF_3SO_3^-Li^+$ triple ions by observing the concentration-dependent changes in Raman spectra of $LiCF_3SO_3$ solution.[11]

Mass spectrometry (MS) has been a versatile technique for investigating ionic clusters, including triple ions in the gas phase. The soft ionization methods, such as electrospray ionization (ESI) and matrix-assisted laser desorption/ ionization (MALDI), efficiently generate triple ions and higher cluster ions from electrolytic solutions containing various ionic species.[14-16] Furthermore, the mass-selection capability of MS allows for the isolation of specific triple ion or their solvated complexes of interest from the ensemble of diverse ionic clusters, which enables the investigation of triple ion-specific solvation processes in the gas phase. Pioneering works on lithium and lithium halide triple ions were made by Shin and coworkers,[6–8] in which stepwise solvations of $Li^+X^-Li^+$ triple ions (X = Cl and Br) in the gas phase with various O-donor Lewis bases were studied using Fourier-transform ion cyclotron resonance (FT-ICR) mass spectrometry. By trapping of $Li^+X^-Li^+$ triple ions in the ICR cell under the presence of background O-donor solvent molecules such as dioxanes, tetrahydrofuran, diethyl ether, and several more, their

binding stoichiometry and thermodynamics in the gas phase were determined in the gas phase. Furthermore, the stable structures of Li^+ and $Li^+X^-Li^+$ complexes with O-donor solvents were suggested by *ab initio* theoretical calculations.

However, the proposed low-energy structures of solvated Li^+ and triple ions have not been confirmed experimentally. The possible existences of structural isomers have not been examined so far. Therefore, we have employed ESI and ion mobility spectrometry-mass spectrometry (IMS-MS) to confirm predicted low-energy structures of Li^+ and $Li^+X^-Li^+$ triple ion solvated by O-donor Lewis bases. Electrospraying electrolyte solutions from atmospheric conditions to the vacuum induces rapid solvent evaporation in which the local electrolyte concentration may instantaneously increase before the complete solvent removal.[17,18] Such conditions can boost the formation of ionic clusters, including triple ions and higher-order cluster ions, making ESI highly beneficial to investigate triple ions in the gas phase using MS. IMS-MS enables us to confirm and distinguish structural isomers by separating molecular ions by their angle-averaged, momentum-transfer collision cross-sections (CCSs) in the gas phase, as the CCS value can be a fingerprint of each isomer, especially for small molecules.

Here, we report the structural determination of Li^+ and $Li^+I^-Li^+$ ions solvated by 1,4-dioxane molecules using ESI-IMS-MS. Since the bidentate binding of two oxygens in 1,4-dioxane requires the conformational transformations between a chair and a (twisted) boat, the various structural isomers are expected for $(1,4\text{-dioxane})_m{\cdot}Li^+$ and $(1,4\text{-dioxane})_m{\cdot}Li^+I^-Li^+$. The existence of structural isomers was confirmed by using IMS, and their structures were revealed with determined CCS values and the density functional theory (DFT) calculations.

Experimental

Materials

1,4-Dioxane and lithium iodide salt (LiI) were purchased from Sigma-Aldrich (St. Louis, MI, USA) and used without further purification. Distilled and deionized water was prepared by an in-lab water purification system (Aquapuri 541, Young In Chromass, South Korea). The LiI sample solution was prepared by dissolving LiI in distilled water to have a concentration of 1 mM. The aqueous 1,4-dioxane solution was also prepared with a concentration of 100 mM.

ESI-ion mobility spectrometry-mass spectrometry

A commercial ion mobility quadrupole time-of-flight (IM-Q-TOF) instrument equipped with an electrospray ionization (ESI) source (6560 IM-Q-TOF, Agilent Technologies Inc., Santa Clara, CA, USA) were used in the present study. The prepared LiI solution was transported to the electrospray emitter with a flow rate of 10 μL min^{-1} and electrosprayed into the inlet capillary under the gentle flow of inlet He gas. The inlet gas supply of the ESI source was slightly modified, as shown in Figure 1. A bubbling jar with dioxane solvents was installed in the inlet gas line to introduce 1,4-dioxane vapors at the cone and inlet capillary regions. The He gas was used to carry 1,4-dioxane vapors since the He environment is supposed to be softer and better than the N_2 atmosphere in order to keep weakly-bound solvated complex ions. Some portion of 1,4-dioxane vapors are released out from the sampling cone to make 1,4-dioxane counterflow, while the remaining portion is transferred into vacuum region together with generated lithium electrolyte ions. The ions in the charged aqueous droplets encounter dioxane vapors during the solvent (water) evaporation process, and therefore the naked Li^+ and $Li^+I^-Li^+$ can form complexes with dioxanes. The generated ions and ion-solvent complexes are trapped at the ion funnel for 50 ms and pulsed into the ~80-cm-log drift tube filled with the nitrogen drift gas (3.94 torr). Ions travel through the drift tube under the presence of a weak electric field (10–15 V cm^{-1}), in which they are separated by their CCS. The orthogonal acceleration TOF was used to record a series of mass spectra in every 160 μs to build a 2D IMS-MS plot with an arrival time and an *m/z* axes. The arrival time distributions (ATDs) of selected ions were extracted from the 2D IMS-MS plot, which were further used to determine their CCS values using the Mason-Schamp equation.[19]

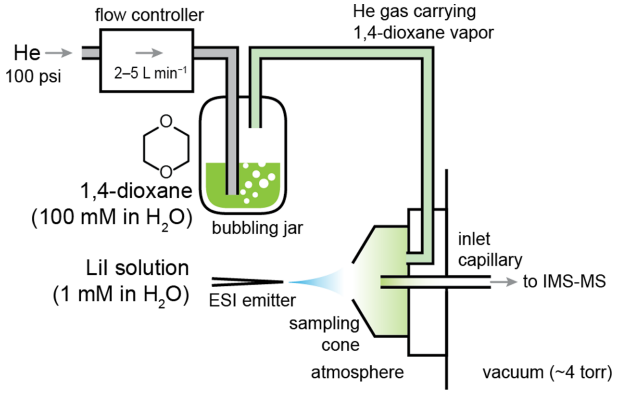

Figure 1. Schematic diagram of the modified ESI inlet which enables inlet gas to carry 1,4-dioxane vapor to the sampling cone. ESI-generated ions can interact with 1,4-dioxane molecules at the inlet region.

Computational Details

The geometries of complexes Li^+ and $Li^+I^-Li^+$ with 1,4-dioxane were optimized at the ωB97xd level of density functional theory (DFT) with def2-TZVPD basis set[20] by using the Gaussian 09 program.[21] The def2-TZVPD basis set is obtained from the Basis Set Exchange (The Molecular Sciences Software Institute, Virginia Tech)[22]

since it is not listed in the basis set library of Gaussian 09. Harmonic vibrational frequencies and zero-point energies were calculated at the same DFT levels and basis set. The Gibbs free energies of 1,4-dioxane bindings were computed at 298 K with counterpoise corrections of basis set superposition error. Partial atomic charges were computed for every atom by performing Hirshfeld population analysis.[23] Theoretical collision cross-section values were calculated for the optimized structures with Hirshfeld atomic charges using the trajectory method[24] implemented in the iMoS program.[25]

Results

The ESI mass spectrum of LiI solution measured with the inlet gas carrying 1,4-dioxane vapor is shown in Figure 2. The bare Li^+ could not be detected in our instrument due to the *m/z* limit of the instrument. The unsolvated $Li^+I^-Li^+$ triple ion is scarcely observed at *m/z* 140.94. At the low-mass region at *m/z* <300, lots of unassigned peaks, presumably from the impurities in the sample and the instrument, dominate the mass spectrum. Nevertheless, precise assessment of the observed monoisotopic mass value allowed us to assign several complex ions of Li^+, $Li^+I^-Li^+$, and 1,4-dioxane molecules accurately with less than 20 ppm relative errors.

Li^+ ions solvated by one and two 1,4-dioxane molecules, $(1,4\text{-dioxane})_m\cdot Li^+$ (m = 1 and 2), are found with moderate abundances at *m/z* 95.0675 and 183.1194, respectively. Their expected monoisotopic *m/z* values are 95.0685 and 183.1209. The $(1,4\text{-dioxane})_3\cdot Li^+$ ion is also observed at *m/z* 271.1677 (expected *m/z* 271.1733) but with very low abundances (Figure 2c). The Li^+ ion with more than three 1,4-dioxane molecules is not observed. The $Li^+I^-Li^+$ triple ions solvated by a 1,4-dioxane molecule, $(1,4\text{-dioxane})_1\cdot Li^+I^-Li^+$, are found at *m/z* 228.9884 with low but observable abundances, while those solvated by two or more 1,4-dioxane molecules are not found. Since iodine has a mass defect distinct from lithium, carbon, and oxygen, the iodine-containing triple ion can be unambiguously observed even with its low abundance.

The ATDs of the solvated Li^+ and $Li^+I^-Li^+$ ions are shown in Figure 3. The singly-solvated Li^+ ions, $(1,4\text{-dioxane})_1\cdot Li^+$, show a broad ATD peak (**1**, ~2.4 ms FWHM) which may represent the presence of multiple

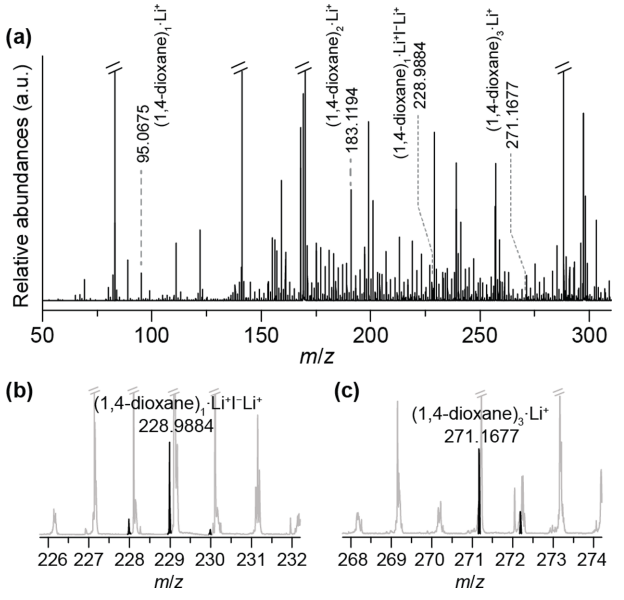

Figure 2. The ESI mass spectrum of LiI solution with the inlet gas carrying 1,4-dioxane vapor: (a) the entire mass spectrum below *m/z* 300; and the blow-up spectra at regions for (b) $(1,4\text{-dioxane})_1\cdot Li^+I^-Li^+$ and (c) $(1,4\text{-dioxane})_1\cdot Li^+$

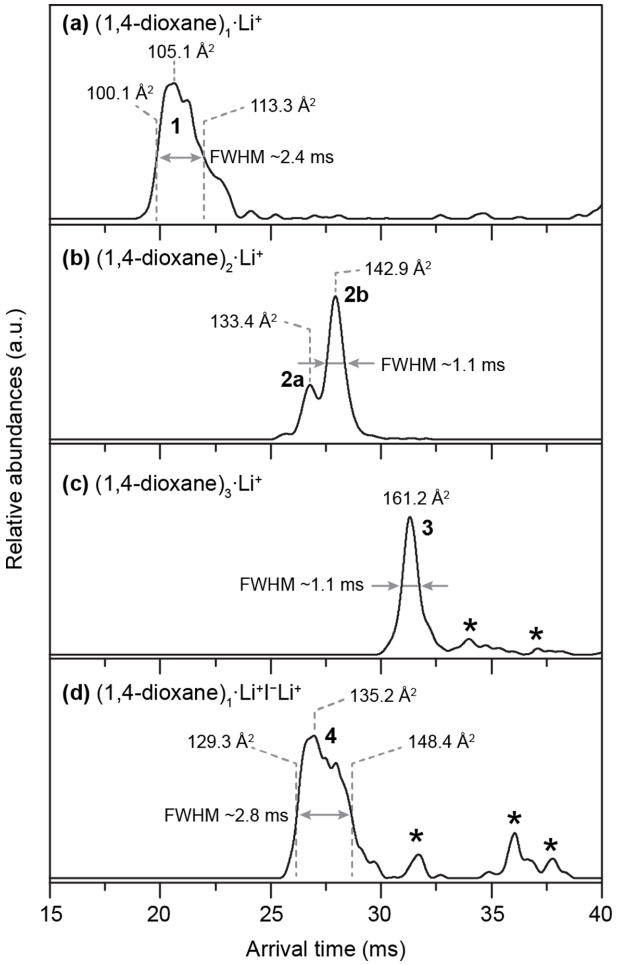

Figure 3. The arrival time distributions (ATDs) of (a) $(1,4\text{-dioxane})_1\cdot Li^+$, (b) $(1,4\text{-dioxane})_2\cdot Li^+$, (c) $(1,4\text{-dioxane})_3\cdot Li^+$, and (d) $(1,4\text{-dioxane})_1\cdot Li^+I^-Li^+$. The determined CCS value is given for each observed ATD feature. Asterisks denote artifact peaks due to the unexpected mass overlaps with low-mass impurities. The ATDs were obtained under the drift electric field of ~10.1 V cm^{-1}.

isomers. Although the limited resolution prevents us from distinguishing isomers clearly and determining their CCS values separately, the CCS values of unresolved isomers are estimated to be at ~105 Å^2 in the range of 100–113 Å^2. In the case of (1,4-dioxane)$_2$·Li^+, two distinguishable ATD features (**2a** and **2b**) with narrow peak width (~1.1 ms FWHM) are observed. The **2b** of the larger CCS value is twice more abundant than the compact **2a**. The determined CCS values are 133.4 and 142.9 Å^2 for **2a** and **2b**, respectively. On the other hand, the (1,4-dioxane)$_3$·Li^+ show a narrow ATD peak (~1.1 ms FWHM) at the arrival times of ~32 ms, suggesting only one isomer (**3**) with a CCS value of 161.2 Å^2. The $Li^+I^-Li^+$ triple ion solvated by a 1,4-dioxane molecule, (1,4-dioxane)$_1$·$Li^+I^-Li^+$, shows multiple partially resolved ATD features (**4**, ~2.8 ms FWHM), suggesting at least two structural isomers of similar abundances. Based on the peak FWHM, the CCS values of unresolved isomers are estimated to fall in the range of 129–148 Å^2.

DFT calculations were performed to find possible low-energy structures and gain further insights into the structural details of observed isomers. Firstly, two low-energy isomers for (1,4-dioxane)$_1$·Li^+ were predicted by DFT calculation (Figure 4a). The most stable isomer of (1,4-dioxane)$_1$·Li^+ has a 1,4-dioxane of a boat conformation, forming bidentate coordination to Li^+ (**B$_1$**). The monodentate isomer between a Li^+ ion and a chair form 1,4-dioxane (**C$_1$**) is ~1.5 kcal mol^{-1} less stable than **B$_1$**. Theoretical CCS values of **B$_1$** and **C$_1$** are 105 Å^2 and 111 Å^2, respectively, which fall within the experimental CCS range of the observed **1** (100–113 Å^2).

Secondly, three low-energy isomers were theoretically optimized for (1,4-dioxane)$_2$·Li^+, which include complex ions with i) two bidentate coordinations (**B$_2$**) with two boat-form 1,4-dioxanes, ii) one bidentate and one monodentate coordinations (**B$_1$C$_1$**) with one boat and one chair conformers, and iii) two monodentate coordinations (**C$_2$**) with two chair conformers (Figure 4b). Interestingly, the **C$_2$** isomer is the most stable, presumably due to the least steric hindrance, but only 2.4 and 2.0 kcal mol^{-1} more stable than **B$_2$** and **B$_1$C$_1$** isomers, respectively. Theoretical CCS values of **B$_2$** (133 Å^2) and **B$_1$C$_1$** (135 Å^2) are similar to each other, while **C$_2$** has a much larger CCS value (144 Å^2). Among two observed ATD features of (1,4-dioxane)$_2$·Li^+, **2a** can be assigned to either **B$_2$** or **B$_1$C$_1$** isomer based on the CCS values. The more extended and abundant **2b** can fit well to the most stable **C$_2$** structure.

Thirdly, three monodentate bindings of chair-form 1,4-dioxane molecules to Li^+ (**C$_3$**) (Figure 4c) were predicted

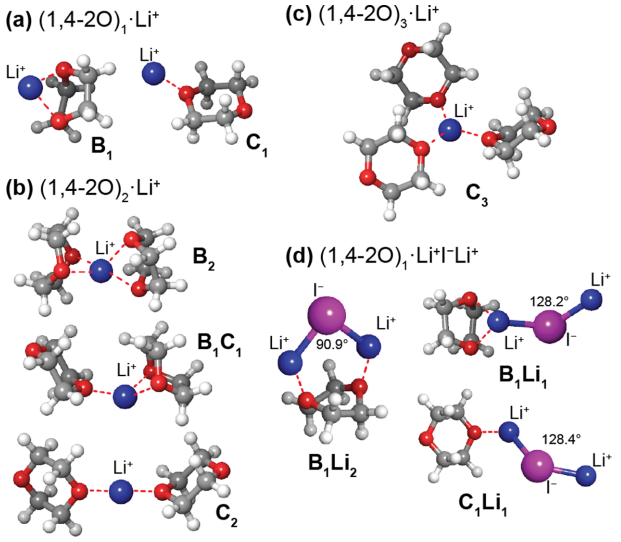

Figure 4. The optimized low-energy structures of solvated Li^+ and $Li^+I^-Li^+$ ions: (a) (1,4-dioxane)$_1$·Li^+, (b) (1,4-dioxane)$_2$·Li^+, (c) (1,4-dioxane)$_3$·Li^+, and (d) (1,4-dioxane)$_1$·$Li^+I^-Li^+$.

Table 1. The relative energetics of the predicted structures for the experimentally observed isomers

complex ion	structure		N_2 CCS (Å^2)		$\Delta G_{298\,K}$[c] (kcal mol^{-1})
	obs.[a]	assg.[b]	obs.	pred.	
(1,4-dioxane)$_1$·Li^+	**1**	**B$_1$**	100.1–113.3	105	−29.7
		C$_1$		111	−28.1
(1,4-dioxane)$_2$·Li^+	**2a**	**B$_2$**	133.3	133	−46.3
		B$_1$C$_1$		135	−46.5
	2b	**C$_2$**	143.1	144	−48.6
(1,4-dioxane)$_3$·Li^+	**3**	**C$_3$**	161.2	165	−72.9
(1,4-dioxane)$_1$·$Li^+I^-Li^+$	**4**	**B$_1$Li$_2$**	129.3–148.4	135	−22.6
		B$_1$Li$_1$		134	−17.2
		C$_1$Li$_1$		138	−19.6

[a] experimentally observed from ATD features in Figure 3
[b] assigned optimized structures in Figure 4 of which CCS values match to the experimental CCS values of observed ATD features
[c] Gibbs free energy of solvent binding at 298 K for the reaction m·1,4-dioxane + $(LiI)_n Li^+ \rightarrow$ (1,4-dioxane)$_m$·$(LiI)_n Li^+$ (n = 0 or 1)

for (1,4-dioxane)$_3$·Li$^+$, in which coordinating three oxygens and Li$^+$ center are located in place. Its theoretical CCS value is 165 Å^2, showing a reasonable agreement to the observed isomer **3** in Figure 3. No bidentate coordination is allowed for (1,4-dioxane)$_3$·Li$^+$ ion, presumably due to the steric hindrance.

Meanwhile, three structures are optimized for the (1,4-dioxane)$_1$·Li$^+$I$^-$Li$^+$ complex (Figure 4d). The most stable and compact isomer is $\mathbf{B_1Li_2}$ with a side-on binding in which two Li atoms bind to each oxygen in a boat-form 1,4-dioxane molecule. Other predicted low-energy isomers have only one Li atom participating in the solvation. The $\mathbf{B_1Li_1}$ and $\mathbf{C_1Li_1}$ isomers have end-on bidentate and monodentate bindings, respectively. This is in line with the previous calculational results for Li$^+$Cl$^-$Li$^+$ and Li$^+$Br$^-$Li$^+$ with a 1,4-dioxane where bidentate end-on, monodentate end-on, and bidentate side-on bindings were predicted.[6,8] Their theoretical CCS values are 135 Å^2 ($\mathbf{B_1Li_2}$), 134 Å^2 ($\mathbf{B_1Li_1}$), and 139 Å^2 ($\mathbf{C_1Li_1}$), which are all in the range of experimental CCS values (129–148 Å^2) for (1,4-dioxane)$_1$·Li$^+$I$^-$Li$^+$ (**4**). The $\mathbf{B_1Li_2}$ with a side-on binding is the most stable among them. The end-on isomers, $\mathbf{B_1Li_1}$ and $\mathbf{C_1Li_1}$, are 5.4 kcal mol^{-1} and 3.0 kcal mol^{-1} less stable than $\mathbf{B_1Li_2}$, respectively.

In summary, the structural isomers of the Li$^+$ and Li$^+$I$^-$Li$^+$ ions solvated by 1,4-dioxane molecules are confirmed experimentally by using IMS-MS, and their structures were revealed with observed CCS values and DFT calculations.

Discussion

Factors determining the stabilities of ion-solvent complex isomers

Two oxygens in a dioxane molecule allow for either monodentate or bidentate coordination to Li$^+$ ion and Li$^+$I$^-$Li$^+$ triple ion. In general, bidentate coordination is energetically more favored than monodentate coordination. However, the bidentate coordination of 1,4-dioxane requires the endothermic conformational transition from the most stable chair form to the less stable boat or twisted boat form, which diminishes its energetic advantage over the monodentate coordination. Therefore, the monodentate and bidentate coordination combinations were predicted to have similar stabilities within 5 kcal mol^{-1} differences, presenting multiple low-energy isomers of Li$^+$ and Li$^+$I$^-$Li$^+$ solvated by 1,4-dioxane molecules.

Steric effects are also significant on the solvation of the small Li$^+$ ion. Due to the small ionic radius of Li$^+$, the coordination of more than four O-donor bases are known to be unfavorable due to the steric effect. Previously, the maximum solvation numbers of Li$^+$ with single O-donor ethers such as tetrahydrofuran, acetone, and diethylether were reported to be three or four.[7] The single bidentate binding occupies already two coordination site of Li$^+$, and therefore more than two bidentate bindings on Li$^+$ is not possible sterically. Furthermore, the bidentated binding of the 1,4-dioxane is not easy to release steric repulsions due to the restricted internal rotaions of dioxane ring geometry. For example, The $\mathbf{C_2}$ conformation of (1,4-dioxane)$_2$·Li$^+$ has a linear O–Li–O bond which minimize the steric hindrance between two dioxanes, allowing the tight Li–O binding with a short bond length (~1.80 Å). Replacing one 1,4-dioxane in $\mathbf{C_2}$ into bidentate coordination, the resulting $\mathbf{B_1C_1}$ has the longer monodentate Li–O bond length (~1.85 Å). This clearly indicates the steric repulsion due to the bidentate binding which occupies large space around the Li$^+$. Furthermore, the $\mathbf{B_2}$ conformation already occupies four possible coordination site of Li$^+$. The optimal may be the tetrahedral coordination, but O–Li–O angles are 74–75° and 120–121°, which are largely deviated from the optimal coordination geometry. However, the restricted internal rotations of rings and the steric repulsions between two bulky dioxanes prevent further stabilizations. These steric effects dictate (1,4-dioxane)$_3$·Li$^+$ to have three monodentate bindings ($\mathbf{C_3}$).

For the Li$^+$I$^-$Li$^+$ triple ion, the bent angle of Li–I–Li is another factor determining the stability of the solvated triple ion. The Li–I–Li angle of the free Li$^+$I$^-$Li$^+$ is predicted as 126.3°. Increasing or decreasing the angle may result in the destabilization of the triple ion. Although the $\mathbf{B_1Li_2}$ isomer has much more stable side-on binding with two paired Li–O coordination than the other isomers ($\mathbf{B_1Li_1}$ and $\mathbf{C_1Li_1}$) with end-on binding, the relatively small Li–I–Li angle (90.9°) to accommodate two paired Li–O coordinations destabilize $\mathbf{B_1Li_2}$ to have similar overall stability with $\mathbf{B_1Li_1}$ and $\mathbf{C_1Li_1}$ which have the Li–I–Li angle (~128°) similar to the free triple ion.

Abundant observations of less-stable isomers: Kinetically trapped solvated ions

In the present results, the relative abundances of the less-stable isomers are more than expected by Boltzmann factors. For example, the $\mathbf{C_2}$ isomer of (1,4-dioxane)$_2$·Li$^+$ is >2 kcal mol^{-1} more stable than $\mathbf{B_2}$ and $\mathbf{B_1C_1}$, suggesting $\mathbf{C_2}$ should be >27 times more abundant than the others. However, the observed abundance of the **2b** peak in ATD is only twice the **2a** peak. Similarly, the observed ATD feature **1** for (1,4-dioxane)$_1$·Li$^+$ is supposed to have multiple isomers with similar relative abundances, although the 1.5 kcal mol^{-1} difference in the energy between $\mathbf{B_1}$ and $\mathbf{C_1}$ structures should yield ~10 times difference in their abundances.

We speculate that the less stable isomer can be formed abundantly during the ESI process and trapped kinetically without undergoing isomerization to the most stable isomer. Unlike the previous FT-ICR studies on Li$^+$Br$^-$Li$^+$ and Li$^+$Cl$^-$Li$^+$ triple ions[6,8] in which those ions are isolated, trapped, and solvated in the ICR cell, ion solvations by 1,4-dioxane molecules in the present work is achieved during

the ESI where H_2O molecules are not entirely removed. Some less-stable isomers may be further stabilized in the presence of attached H_2O molecules, and they have chances to survive as 'kinetically trapped' species during the measurement.

Furthermore, the formation of the Li^+-solvent complex is known to involve the ion-molecule collisions which may lead to the formation of the thermally activated collision complex.[8] The formations of less-stable isomers are eligible under such activated conditions, and therefore sufficient time delay is mandatory to undergo thermal and structural relaxation to reach the most stable isomer. Previous studies on the stepwise Li^+ solvation in the ICR cell suggested the lifetime of the thermally activated collision complex between a Li^+ ion and O-donor solvent molecules is in the several hundreds milliseconds scale, which is longer than the entire timescale of the IMS-MS measurement. Therefore, a significant kinetic shift is expected in the present work compared to the ICR studies with a much longer timescale (>1 s). Even after the complete removal of H_2O solvent, a few milliseconds might not be enough to undergo the structural rearrangement to the most stable isomer. These circumstances enable less stable isomers to survive during the IMS-MS and to be observed.

Implications on investigating stepwise solvation process of lithium electrolyte ions

Previous studies on the stepwise solvation of lithium electrolyte cations did not take the presence of multiple isomers into account. Although *ab initio* calculations predicted the multiple isomers for Li^+–solvent and $Li^+X^-Li^+$–solvent complexes, the measured kinetic and thermodynamic parameters were not isomer-specific. The presence of structural isomers becomes more significant for the bidentate Lewis base solvents such as 1,4-dioxane which can undergo conformational transitions and present multiple binding geometries. Therefore, the stepwise solvation process of lithium electrolyte ion is not a simple one-way sequential reaction but should be treated as a multiply-branched reaction which can lead to several different isomers. The present results that confirm structural isomers with different solvent binding energetics and geometries strongly suggest that the isomer-specific study is necessary for understanding accurate and complete solvation kinetics of lithium electrolyte ions.

Conclusions

The IMS-MS was employed to observe the structural isomers of Li^+ ions and $Li^+I^-Li^+$ triple ions solvated by bidentate O-donor Lewis base, 1,4-dioxane, in the gas phase. DFT calculation together with the determined CCS values successfully revealed the detailed structure of each isomer. The formations of multiple low-energy isomers are attributed to the conformational flexibility (the chair-boat transition) of 1,4-dioxane which determines monodentate or bidentate bindings to the Li^+ or $Li^+I^-Li^+$ ion. The present result further suggests that the isomer-specific study on the solvation kinetics and energetics are necessary to gain precise insights into the ion solvation with bidentate O-donor Lewis bases such as 1,4-dioxane, calling for the further experimental approach which combines IMS and trapping mass analyzer for precise measurement of isomer-specific solvation study in the gas phase.

Supplementary Information

Supplementary information is available at https://drive.google.com/file/d/1Jk0A98zcwHwnuQefm7Vegd8lA8EU1v4T/view?usp=sharing.

Acknowledgments

The authors are grateful for the financial support from the National Research Foundation (NRF) (grant No. 2019R1C1C1008414 and 2020R1A5A1019141), funded by the Ministry of Science and ICT (MSIT). Y.C. thanks to the support from Brain Korea 21 FOUR (Fostering Outstanding Universities for Research) program funded by the Ministry of Education (MOE) and NRF.

References

1. Friedman, H. L. *Annu. Rev. Phys. Chem.* **1981,** 32, 179, DOI: 10.1146/annurev.pc.32.100181.001143.
2. Rossky, P. J.; Dudowicz, J. B.; Tembe, B. L.; Friedman, H. L. *J. Chem. Phys.* **1980,** 73, 3372, DOI: 10.1063/1.440533.
3. Mochizuki, S.; Wakisaka, A. *J. Phys. Chem. A* **2002,** 106, 5095, DOI: 10.1021/jp014583q.
4. Xu, K. *Chem. Rev.* **2004,** 104, 4303, DOI: 10.1021/cr030203g.
5. Hyun, J.-K.; Dong, H.; Rhodes, C. P.; Frech, R.; Wheeler, R. A. *J. Phys. Chem. B* **2001,** 105, 3329, DOI: 10.1021/jp003591o.
6. Jarek, R.; Denson, S. C.; Shin, S. K. *J. Chem. Phys.* **1998,** 109, 4258, DOI: 10.1063/1.477031.
7. Jarek, R. L.; Miles, T. D.; Trester, M. L.; Denson, S. C.; Shin, S. K. *J. Phys. Chem. A* **2000,** 104, 2230, DOI: 10.1021/jp9908193.
8. Jarek, R. L.; Shin, S. K. *J. Am. Chem. Soc.* **1997,** 119, 10501, DOI: 10.1021/ja971841h.
9. Khartabil, H. K.; Gros, P. C.; Fort, Y.; Ruiz-López, M. F. *J. Org. Chem.* **2008,** 73, 9393, DOI: 10.1021/jo8019434.
10. Ohtani, H.; Hirao, Y.; Ito, A.; Tanaka, K.; Hatozaki, O. *J. Therm. Anal. Calorim.* **2010,** 99, 139, DOI: 10.1007/s10973-009-0520-7.
11. Petersen, G.; Jacobsson, P.; Torell, L. M. *Electrochim. Acta* **1992,** 37, 1495, DOI: 10.1016/0013-4686(92)80097-6.
12. Tretyakov, D. O.; Prisiazhnyi, V. D.; Gafurov, M. M.;

Rabadanov, K. S.; Kirillov, S. A. *J. Chem. Eng. Data* **2010,** 55, 1958, DOI: 10.1021/je9009249.
13. Ziegler, M. J.; Madura, J. D. *J. Solution Chem.* **2011,** 40, 1383, DOI: 10.1007/s10953-011-9732-0.
14. Ahonen, L.; Li, C.; Kubečka, J.; Iyer, S.; Vehkamäki, H.; Petäjä, T.; Kulmala, M.; Hogan Jr, C. J. *J. Phys. Chem. Lett.* **2019,** 10, 1935, DOI: 10.1021/acs.jpclett.9b00453.
15. Calabrese, V.; Lavanant, H.; Rosu, F.; Gabelica, V.; Afonso, C. *J. Am. Soc. Mass Spectrom.* **2020,** 31, 969, DOI: 10.1021/jasms.0c00034.
16. Ouyang, H.; Larriba-Andaluz, C.; Oberreit, D. R.; Hogan, C. J. *J. Am. Soc. Mass Spectrom.* **2013,** 24, 1833, DOI: 10.1007/s13361-013-0724-8.
17. Wei, Z.; Li, Y.; Cooks, R. G.; Yan, X. *Annu. Rev. Phys. Chem.* **2020,** 71, 31, DOI: 10.1146/annurev-physchem-121319-110654.
18. Rovelli, G.; Jacobs, M. I.; Willis, M. D.; Rapf, R. J.; Prophet, A. M.; Wilson, K. R. *Chem. Sci.* **2020,** 11, 13026, DOI: 10.1039/d0sc04611f.
19. Mason, E. A.; McDaniel, E. W., *Transport Properties of Ions in Gases*. Wiley: 1988, DOI: 10.1002/3527602852.
20. Weigend, F. *Phys. Chem. Chem. Phys.* **2006,** 8, 1057, DOI: 10.1039/b515623h.
21. Frisch, M. J.; Trucks, G. W.; Schlegel, H. B.; Scuseria, G. E.; Robb, M. A.; Cheeseman, J. R.; Scalmani, G.; Barone, V.; Petersson, G. A.; Nakatsuji, H.; Li, X.; Caricato, M.; Marenich, A.; Bloino, J.; Janesko, B. G.; Gomperts, R.; Mennucci, B.; Hratchian, H. P.; Ortiz, J. V.; Izmaylov, A. F.; Sonnenberg, J. L.; Williams-Young, D.; Ding, F.; Lipparini, F.; Egidi, F.; Goings, J.; Peng, B.; Petrone, A.; Henderson, T.; Ranasinghe, D.; Zakrzewski, V. G.; Gao, J.; Rega, N.; Zheng, G.; Liang, W.; Hada, M.; Ehara, M.; Toyota, K.; Fukuda, R.; Hasegawa, J.; Ishida, M.; Nakajima, T.; Honda, Y.; Kitao, O.; Nakai, H.; Vreven, T.; Throssell, K.; Jr., J. A. M.; Peralta, J. E.; Ogliaro, F.; Bearpark, M.; Heyd, J. J.; Brothers, E.; Kudin, K. N.; Staroverov, V. N.; Keith, T.; Kobayashi, R.; Normand, J.; Raghavachari, K.; Rendell, A.; Burant, J. C.; Iyengar, S. S.; Tomasi, J.; Cossi, M.; Millam, J. M.; Klene, M.; Adamo, C.; Cammi, R.; Ochterski, J. W.; Martin, R. L.; Morokuma, K.; Farkas, O.; Foresman, J. B.; Fox, D. J., Gaussian 09, Revision A.02. Gaussian, Inc.: Wallingford CT, 2016.
22. Pritchard, B. P.; Altarawy, D.; Didier, B.; Gibson, T. D.; Windus, T. L. *J. Chem. Inf. Model.* **2019,** 59, 4814, DOI: 10.1021/acs.jcim.9b00725.
23. Ritchie, J. P.; Bachrach, S. M. *J. Comput. Chem.* **1987,** 8, 499, DOI: 10.1002/jcc.540080430.
24. Mesleh, M. F.; Hunter, J. M.; Shvartsburg, A. A.; Schatz, G. C.; Jarrold, M. F. *J. Phys. Chem.* **1996,** 100, 16082, DOI: 10.1021/jp961623v.
25. Coots, J.; Gandhi, V.; Onakoya, T.; Chen, X.; Larriba-Andaluz, C. *J. Aerosol Sci.* **2020,** 147, 105570, DOI: 10.1016/j.jaerosci.2020.105570.

